

Constraining the chlorine monoxide (ClO)/chlorine peroxide (ClOOCl) equilibrium constant from Aura Microwave Limb Sounder measurements of nighttime ClO

Michelle L. Santee, Stanley P. Sander¹, Nathaniel J. Livesey, and Lucien Froidevaux

Jet Propulsion Laboratory, California Institute of Technology, Pasadena, CA

Edited by Barbara J. Finlayson-Pitts, University of California, Irvine, Irvine, CA, and approved February 22, 2010 (received for review November 2, 2009)

The primary ozone loss process in the cold polar lower stratosphere hinges on chlorine monoxide (ClO) and one of its dimers, chlorine peroxide (ClOOCl). Recently, analyses of atmospheric observations have suggested that the equilibrium constant, K_{eq} , governing the balance between ClOOCl formation and thermal decomposition in darkness is lower than that in the current evaluation of kinetics data. Measurements of ClO at night, when ClOOCl is unaffected by photolysis, provide a useful means of testing quantitative understanding of the ClO/ClOOCl relationship. Here we analyze nighttime ClO measurements from the National Aeronautics and Space Administration Aura Microwave Limb Sounder (MLS) to infer an expression for K_{eq} . Although the observed temperature dependence of the nighttime ClO is in line with the theoretical ClO/ClOOCl equilibrium relationship, none of the previously published expressions for K_{eq} consistently produces ClO abundances that match the MLS observations well under all conditions. Employing a standard expression for K_{eq} , $A \times \exp(B/T)$, we constrain the parameter A to currently recommended values and estimate B using a nonlinear weighted least squares analysis of nighttime MLS ClO data. ClO measurements at multiple pressure levels throughout the periods of peak chlorine activation in three Arctic and four Antarctic winters are used to estimate B . Our derived B leads to values of K_{eq} that are ~ 1.4 times smaller at stratospherically relevant temperatures than currently recommended, consistent with earlier studies. Our results are in better agreement with the newly updated (2009) kinetics evaluation than with the previous (2006) recommendation.

Current understanding of ozone loss in the polar lower stratosphere holds that photolysis of one of the chlorine monoxide (ClO) dimers, chlorine peroxide (ClOOCl), is the rate-limiting step in the ClO + ClO catalytic cycle of ozone destruction (1). In darkness, when ClO and ClOOCl should be in equilibrium, partitioning between them is governed by the equilibrium constant, K_{eq} , defined to be the ratio of the rate constants of the ClO self-reaction that forms ClOOCl ($\text{ClO} + \text{ClO} + \text{M} \rightarrow \text{ClOOCl} + \text{M}$, where M is a third body) and the ClOOCl thermal dissociation reaction ($\text{ClOOCl} + \text{M} \rightarrow \text{ClO} + \text{ClO} + \text{M}$). Thus $K_{\text{eq}} = [\text{ClOOCl}]/[\text{ClO}]^2$ when ClOOCl and ClO are in thermal equilibrium; i.e., photolysis is negligible and sufficient time has elapsed for equilibrium to have been achieved. K_{eq} is strongly temperature-dependent; at higher temperatures (above ~ 200 K), ClOOCl decomposes and ClO is favored.

All laboratory determinations of K_{eq} to date have been conducted at temperatures considerably above those relevant for the lower stratospheric winter polar vortices. Recent reports from the National Aeronautics and Space Administration (NASA) Data Evaluation Panel, including the widely used JPL06 recommendation (2), have extrapolated experimental values to lower stratospheric conditions. Questions have been raised, however, about the realism of the extrapolated values. Brune et al. (3) observed substantial ClO abundances at high solar zenith angles and estimated the magnitude of chlorine activation on the basis of thermal equilibrium between ClO and ClOOCl; their analysis

suggested a lower value of K_{eq} than that determined in a previous laboratory study (4). Since then, several other studies based on atmospheric observations, from both in situ (5–10) and satellite (11) sensors, have also concluded that considerably smaller values of K_{eq} (implying a lower temperature at which thermal decomposition overtakes photolysis as the dominant ClOOCl loss process at high solar zenith angles) are needed to match observed nighttime ClO. Recent laboratory measurements (12, 13) support smaller values for K_{eq} as well, although these studies did not measure K_{eq} directly. The latest evaluation, JPL09 (14), a partial update produced in support of the upcoming 2010 World Meteorological Organization Scientific Assessment of Ozone Depletion, also recommends a K_{eq} smaller than that in JPL06. The NASA Data Panel recommendations in JPL06 and JPL09 are based solely on studies providing direct measurements of K_{eq} (4, 15), with the differences between the JPL06 and JPL09 expressions arising primarily from a change in the weighting applied to laboratory measurements of K_{eq} at low temperature. Overall, values of K_{eq} reported in the literature vary by a factor of 2 at 298 K (and by larger factors at lower temperatures; e.g., ref. 13). Smaller values of K_{eq} imply greater thermal dissociation of ClOOCl, resulting in more ClO at a given temperature but less ClOOCl available to photolyze and consequently less chlorine-catalyzed ozone destruction, particularly in twilight. Better knowledge of K_{eq} is therefore required for accurate prediction of polar ozone loss, especially in the Arctic, where polar vortex temperatures frequently fall in the regime within which both photolysis and thermal decomposition of ClOOCl control net ClO abundances.

The Microwave Limb Sounder (MLS), launched as part of NASA's Aura mission in July 2004, measures vertical profiles of a suite of trace gases in the middle atmosphere, including ClO. MLS provides daily global coverage, allowing the behavior of ClO to be investigated over a broad range of temperatures throughout the polar vortices for multiple winters in both hemispheres. Here we exploit the vast quantity of MLS data available to constrain the value of K_{eq} , first by comparing MLS measurements of nighttime ClO to equilibrium ClO abundances predicted using selected forms of K_{eq} from the literature, and then by inferring K_{eq} from the MLS nighttime ClO observations themselves under the assumption that the equilibrium relationship between ClO and ClOOCl controls ClO abundances in darkness.

Aura MLS Observations of Nighttime ClO

Chlorine activation leads to substantial ClO enhancement at polar latitudes throughout the lower stratosphere during winter in both hemispheres (1). Fig. 1 shows MLS nighttime ClO data

Author contributions: M.L.S., S.P.S., N.J.L., and L.F. designed research; M.L.S., N.J.L., and L.F. performed research; M.L.S., S.P.S., N.J.L., and L.F. analyzed data; and M.L.S. wrote the paper.

The author declares no conflict of interest.

This article is a PNAS Direct Submission.

¹To whom correspondence should be addressed. E-mail: Stanley.P.Sander@jpl.nasa.gov.

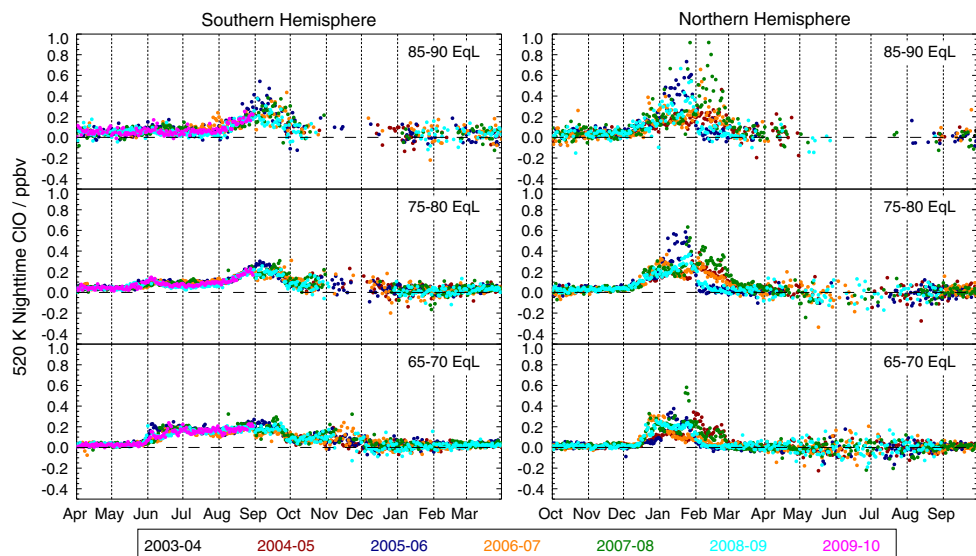


Fig. 1. Time series of bias-corrected (25; also see *Methods*) version 2.2 nighttime MLS ClO at 520 K potential temperature (~ 46 hPa, ~ 19 km) for the Southern (*Left*) and Northern (*Right*) Hemispheres. Daily means were calculated by binning nighttime data (i.e., having local SZA $> 105^\circ$) into 5° -wide bands of EqL and averaging; selected representative bins are shown. Different years are represented by different colors as indicated in the legend. Dashed vertical lines demarcate calendar months.

interpolated to 520 K potential temperature (~ 46 hPa, ~ 19 km altitude) near the peak in the ClO vertical profile. Daily averages are calculated in equivalent latitude [EqL, the latitude encircling the same area as a given contour of potential vorticity (16)], rather than geographic latitude, to obtain a polar vortex-centered view. This approach ensures that only meteorologically similar air masses are averaged together and that regions of ClO enhancement inside the winter polar vortex are segregated from extravortex regions, where ClO mixing ratios are generally very low. MLS observes nonnegligible nighttime enhancement in ClO poleward of 60 – 65° EqL in all winters, from late May through September in the Antarctic, and from December through February in the Arctic. EqL-mean values at night approach 1 part per billion by volume (ppbv) in the Arctic midwinter. Although in general the magnitude of chlorine activation is considerably greater in the Antarctic (1), lower midwinter temperatures there typically lead to ClO enhancements in darkness smaller than those observed in the Arctic. Greater variability in nighttime ClO abundances in the Arctic most likely arises because of larger, more frequent temperature fluctuations than in the Antarctic. Scatter increases in both hemispheres during summer, when fewer points are available to contribute to the daily averages.

For the remainder of this analysis we focus only on those measurements identified to lie inside the polar vortex core, conservatively defined by EqL contours of 70° in the Arctic and 65° in the Antarctic. We further focus on the periods of peak chlorine

activation, when most of the chlorine has been converted into reactive forms, and reservoir species such as HCl and ClONO₂ can be assumed to play a minor role. On the basis of previous studies using Aura MLS and model simulations (17) (and similar results for other winters), we define the peak activation periods to encompass January 20 through February 20 in the Arctic and June 25 through September 1 in the Antarctic, during which total reactive chlorine typically constitutes more than 75% (90%) of total inorganic chlorine in the Arctic (Antarctic) lower stratospheric vortex core.

Observed and Calculated Equilibrium ClO Values

Three representative days during the 2008 Arctic winter on which MLS sampled a broad range of temperature conditions inside the vortex core are highlighted in Fig. 2. As expected from ClOCl thermal decomposition, MLS nighttime ClO abundances inside the winter polar vortices generally increase with increasing temperature.

MLS measurements of ClO are compared to equilibrium ClO abundances calculated using selected expressions for K_{eq} from the literature, including the one in the JPL06 recommendation (2) and those derived from in situ atmospheric observations obtained during campaigns in the 1990 (6) and 2003 (8) Arctic winters. These selected sources essentially bracket the range of published K_{eq} values; thus they provide a convenient means of investigating the temperature dependence of the observations and exploring variations in the magnitude of K_{eq} . An alternative,

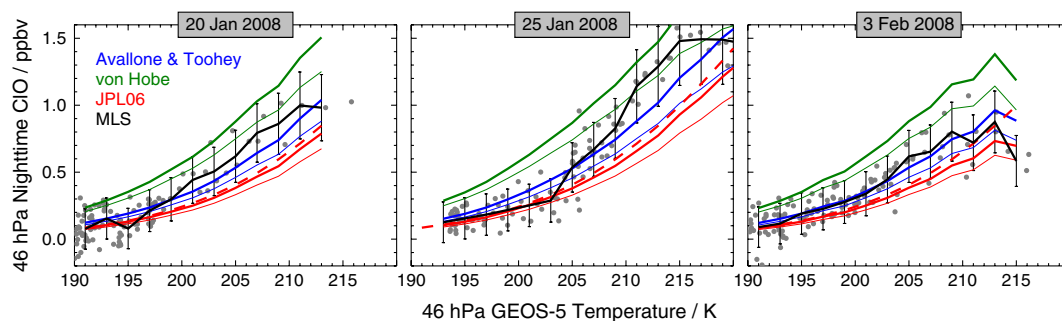


Fig. 2. Individual MLS measurements of nighttime (SZA $> 105^\circ$) ClO inside the Arctic vortex core at 46 hPa (gray dots) as a function of temperature for representative days in the 2008 Arctic midwinter. Thick black lines show the MLS data averaged in 2-K temperature bins, with error bars marking the ClO measurement systematic uncertainty envelope. Thick colored lines show equilibrium ClO abundances calculated using estimates of ClO_x from daily SLIMCAT simulations and the K_{eq} expressions from JPL06 (2, red), Avallone and Toohey (6, blue), and von Hobe et al. (8, green). Equilibrium ClO abundances obtained by reducing the assumed ClO_x by 30% are given by corresponding thin colored lines. Also shown (red dashed lines) are theoretical equilibrium ClO curves based on the JPL06 K_{eq} and a fixed ClO_x abundance of 3.0 ppbv.

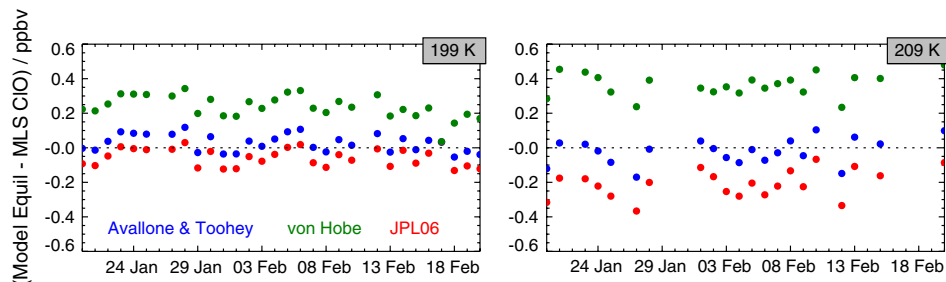


Fig. 3. Time series of the differences between equilibrium ClO abundances estimated using selected K_{eq} expressions (as in Fig. 2) and nominal SLIMCAT ClO_x amounts and ClO abundances measured by MLS over the peak chlorine activation period in the 2008 Arctic winter. Results are shown for the 199-K and 209-K temperature bins at 46 hPa.

essentially equivalent, approach would have been to simply vary the JPL06 parameterization over the range of its reported uncertainty. In any case, it is important to note that, given their large absolute uncertainties, it is not possible to identify one “best” expression for K_{eq} from among those previously published.

Calculation of equilibrium ClO based on a given K_{eq} requires knowledge of the abundance of active chlorine, ClO_x, defined here as ClO + 2 × ClOOCl. Unfortunately, MLS does not measure ClOOCl, and no simultaneous, colocated ClOOCl data exist. Although ClO_x could be inferred from MLS measurements of daytime ClO (17, 18), current uncertainties in the ClOOCl photolysis rate (19–21) compromise the fidelity of such a calculation. Alternatively, ClO_x could be derived by estimating the total inorganic chlorine from MLS measurements of N₂O and assuming complete activation, but this approach introduces errors from the assumed correlation between N₂O and total chlorine as well as from the quality of the MLS N₂O data. Instead, we have chosen to rely on simulated ClO_x values from the SLIMCAT three-dimensional chemical transport model (22). SLIMCAT offers an especially convenient option because customized simulations are available for nearly every day of data, sampled at the MLS locations and times. SLIMCAT has been used extensively for a wide range of studies and in particular has been shown to broadly reproduce polar chemical and dynamical processes (22–24).

Fig. 2 shows that the temperature dependence of MLS ClO is in line with the theoretical ClO/ClOOCl equilibrium relationship. Because of uncertainty in both the measurements and the model curves, it is not possible to unequivocally exclude the existence of other chlorine reservoirs besides ClOOCl, but the results of Fig. 2 arguably preclude any mechanism with a greatly dissimilar temperature dependence. As noted previously (6), it is difficult to distinguish between the various K_{eq} expressions at the lowest temperatures, whereas the measurements at higher temperatures provide a more effective constraint. Variability is significant, with the best correspondence with MLS data obtained for different K_{eq} expressions at different times and temperatures (and pressures). For example, on January 20 none of the expressions provide a particularly good match to the data, although the ClO amounts calculated from the Avallone and Toohey (6) expression are at least within the MLS uncertainty envelope. In contrast, on January 25 the JPL06 K_{eq} leads to equilibrium ClO abundances that initially follow the observed temperature variation well but depart substantially from the data at higher temperatures, where the MLS measurements fall between the curves based on the Avallone and Toohey and von Hobe et al. (8) K_{eq} expressions. On February 3, the K_{eq} from Avallone and Toohey produces good agreement with the data throughout most of the tempera-

ture domain. On all days, the K_{eq} derived by von Hobe et al. overestimates the observed nighttime ClO.

A complication arising from the use of SLIMCAT is that, in part because of the simplified equilibrium scheme used to parameterize polar stratospheric clouds (PSCs), the commonly used version of the model overestimates the magnitude and spatial extent of chlorine activation inside the winter polar vortices, especially at the margins of the PSC season in the Arctic (17). In a typical Antarctic winter, SLIMCAT overestimates ClO_x during the peak chlorine activation period by as much as ~25%, whereas the degree of overestimation during the Arctic midwinter ranges over ~15–50% in much of the lower stratosphere (17). To account for the model overestimation of chlorine activation, we repeated the equilibrium ClO calculations with SLIMCAT ClO_x abundances decreased by 30%, a representative (albeit pessimistic, particularly in the Antarctic) factor. In the reduced-ClO_x scenario, equilibrium abundances derived from the JPL06 K_{eq} substantially underestimate observed ClO at most temperatures (Fig. 2), and agreement with calculations based on the Avallone and Toohey K_{eq} is degraded in most cases. ClO values estimated using the von Hobe et al. K_{eq} , originally far outside the uncertainty envelope of the MLS data, now fall within it for the most part. Results are thus significantly influenced by the assumed ClO_x abundances.

Fig. 3 shows time series over the 2008 Arctic winter peak activation period of the differences between the ClO calculated using the various K_{eq} relationships (based on nominal SLIMCAT ClO_x abundances) and that observed by MLS for two particular temperature bins (199 and 209 K). Despite substantial day-to-day variability in the agreement between modeled and measured ClO, some general conclusions can be drawn. The von Hobe et al. K_{eq} uniformly overestimates MLS ClO. The Avallone and Toohey K_{eq} typically overestimates MLS ClO at the lower temperatures, but often produces the value closest to that observed, whereas JPL06 typically underestimates MLS ClO, but also often agrees with the data most closely. Differences from MLS are generally larger at higher temperatures. None of the K_{eq} expressions consistently provides the best match to MLS ClO data under all conditions.

K_{eq} Estimated from Aura MLS ClO Data

Measurements of ClO in darkness, when photolysis is negligible and remotely sensed air masses are expected to be in chemical and thermal equilibrium, can be used to deduce K_{eq} . MLS covers most of the polar vortex throughout multiple winters in both hemispheres, leading to a vast quantity (tens of thousands) of nighttime ClO measurements over a broader range of temperatures and more diverse conditions than are typically sampled by in situ datasets.

Table 1. Weighted averages of Arctic daily B retrievals

Year	32 hPa (# points)	46 hPa (# points)	68 hPa (# points)	100 hPa (# points)
2005	8,787 ± 183 (3,261)	8,663 ± 43 (3,282)	8,669 ± 50 (3,666)	8,615 ± 79 (3,448)
2007	8,911 ± 156 (2,864)	8,698 ± 42 (2,987)	8,710 ± 42 (3,048)	8,683 ± 65 (2,867)
2008	8,804 ± 122 (2,979)	8,714 ± 37 (3,089)	8,709 ± 38 (3,045)	8,660 ± 72 (2,761)

Table 2. Weighted averages of Antarctic daily B retrievals

Year	32 hPa (# points)	46 hPa (# points)	68 hPa (# points)	100 hPa (# points)
2005	8,637 ± 44 (2,453)	8,681 ± 61 (2,818)	8,644 ± 101 (4,798)	8,598 ± 113 (11,580)
2006	8,653 ± 49 (2,292)	8,726 ± 74 (2,855)	8,682 ± 100 (5,168)	8,508 ± 134 (12,462)
2007	8,640 ± 46 (1,513)	8,622 ± 60 (1,730)	8,692 ± 162 (3,045)	8,708 ± 123 (5,591)
2008	8,639 ± 61 (1,816)	8,787 ± 78 (2,678)	8,743 ± 77 (4,995)	8,660 ± 96 (12,437)

The temperature dependence of the equilibrium constant is often parameterized (2) by an expression of the following form: $K_{\text{eq}} = A \times \exp(B/T)$. Parameter A is related to the standard reaction entropy change, while parameter B is related to the standard reaction enthalpy change, which is equivalent to the O—O bond dissociation energy of ClOOCl at 298 K. We have chosen to deduce K_{eq} using a third law analysis in which the entropy is assumed to be known. Thus we fix the value of A and estimate the value of B . A is first taken to be the value specified in JPL06 ($9.30 \times 10^{-28} \text{ cm}^3 \text{ molecule}^{-1}$); the calculations are then repeated using the updated value ($1.72 \times 10^{-27} \text{ cm}^3 \text{ molecule}^{-1}$) in JPL09 (14).

As before, we take ClO_x abundances from SLIMCAT simulations associated with each MLS measurement point. Only those measurements inside the vortex for which the temperature exceeds 190 K and the solar zenith angle (SZA) exceeds 105° are considered, to ensure that the sampled air parcels have experienced warm conditions and have achieved thermal and chemical equilibrium. With these assumptions, we employ a standard weighted (by the precision on each MLS ClO data point) nonlinear least squares iterative approach that solves for the B value that minimizes the differences between observed and calculated equilibrium ClO on each day. This method yields several advantages over fitting a straight line to the expression $\ln([\text{ClOOCl}]/[\text{ClO}]^2) = \ln(A) + B(1/T)$. In particular, the latter approach requires that the ~0.1 ppbv noise on individual MLS ClO measurements (25) be propagated into $\ln(K_{\text{eq}})$ space. The asymmetry this causes in the error statistics, and the additional complications that arise in taking the logarithm of negative numbers (which occur when measurement noise produces values of ClO exceeding the estimated ClO_x), introduce significant (tens of K) biases into the estimate of B . This bias is avoided in our approach, in which the fit is performed in ClO mixing ratio space, where the noise is Gaussian. MLS radiance noise occasionally gives rise to negative ClO mixing ratios; though unphysical, negative values must be retained to avoid introducing biases into the calculations. B values are retrieved at four MLS retrieval pressure surfaces (32, 46, 68, and 100 hPa) for each day throughout the peak chlorine activation periods (defined previously) in three Arctic (2005, 2007, and 2008) and four Antarctic (2005, 2006, 2007, and 2008) winters. The 2006 and 2009 Arctic winters

are excluded because major stratospheric sudden warmings prematurely terminated polar processing in those winters.

Averages of the daily B values, weighted by their uncertainty arising from ClO measurement noise, are tabulated (based on the JPL06 A) for each pressure surface in each winter in the Arctic (Table 1) and Antarctic (Table 2), along with the number of MLS measurements going into the analysis in each case. We report the uncertainty in these weighted averages as the root mean square of the deviations from the weighted mean, rather than the estimated precision of the mean due to measurement noise (which is much smaller), to capture systematic uncertainties that can vary from day to day. With the exception of the Arctic at 32 hPa, for which the weighted-average B is higher in all winters than for any other cases, no systematic differences with pressure, year, or hemisphere are evident.

With the abundance of MLS data available, we have the luxury of focusing on those pressure levels exhibiting the least scatter in the daily values in all winters: 32 and 46 hPa in the Antarctic and 46 and 68 hPa in the Arctic. Daily B retrievals at these levels are shown for all winters considered in both hemispheres in Fig. 4. As before, some day-to-day variability is evident, especially in the Antarctic. Colder conditions in the Antarctic result in a more limited temperature range being sampled and fewer observations meeting the selection criteria, leading to greater variability and larger error bars than in the Arctic. No substantial trend over the chlorine activation season is seen for any pressure level/winter.

Several different strategies can be used to determine an overall B value. Taking the weighted average of the daily retrievals for the levels and winters depicted in Fig. 4, we find an overall average value of B of $8,685 \pm 77 \text{ K}$. Alternatively, we have also run the retrieval system on the aggregate dataset comprised of all 37,272 MLS measurements of nighttime ClO contributing to the daily retrievals. The value of B retrieved from the combined dataset is 8,694 K, negligibly different from that obtained by averaging the daily retrievals. In either case, the number of data points is sufficiently large that the uncertainty on the estimated B arising solely from noise on the ClO measurements is ~1 K.

Several sensitivity studies have been performed to more fully assess the systematic uncertainties in our retrieved B , as summarized in Table 3. These sensitivity tests were done in the context of the daily retrievals (the majority using the 2008 Arctic winter as a

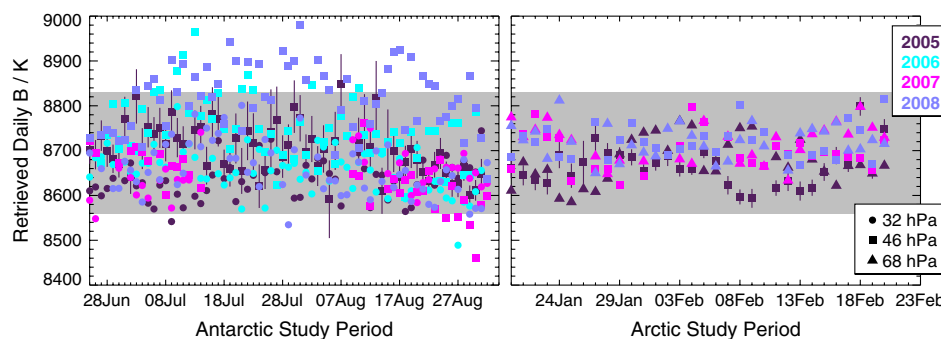


Fig. 4. Time series of daily B retrievals over the four Antarctic (three Arctic) midwinter study periods on the 32 and 46 hPa (46 and 68 hPa) MLS retrieval pressure levels. Parameter A is fixed to the value specified in JPL06 for these retrievals. Error bars are shown for the 46-hPa level for the Arctic and Antarctic winters of 2005 (other error bars omitted for clarity); they reflect the estimated precision of the daily B retrievals, calculated by propagating the precision of the MLS ClO measurements through the retrieval system. Gray shading marks the range around the B value (8,694 K) retrieved from the aggregate dataset arising from its estimated uncertainty ($\pm 135 \text{ K}$). See text for details.

Table 3. Summary of *B* retrieval sensitivity tests

Description of sensitivity tests	ΔB
Using four pressure levels (32, 46, 68, 100 hPa) in each hemisphere, rather than two	+9 K (0.1%)
Using data from the Arctic only (46, 68 hPa)	+12 K (0.1%)
Using data from the Antarctic only (32, 46 hPa)	-23 K (0.3%)
Using SZA > 115° (rather than 105°) to identify “nighttime” MLS ClO measurements*	-12 K (0.1%)
Using T > 195 K (rather than 190 K) to identify MLS measurements in warm conditions*	-3 K (<0.1%)
Considering a 30% overestimation of SLIMCAT ClO _x abundances*	-80 K (0.9%)
Considering a potential error of ±1 K in the GEOS-5 temperature*	±45 K (0.5%)
Considering the uncertainty in the version 2 MLS ClO data (±0.05 ppbv bias, ±10% scaling uncertainty, 1-σ)*	±80 K (0.9%)
Considering a ±0.05 ppbv uncertainty in the latitude- and altitude-dependent version 2 MLS ClO bias correction*	±55 K (0.6%)

*Test run for the 2008 Arctic winter.

test case), rather than on retrievals of the aggregate dataset. Including the daily retrieved values from all four pressure levels in both hemispheres, instead of just two, leads to an overall *B* that is negligibly different (8,694 K) but characterized by a larger root mean square of the deviations from the weighted mean (±115 K, based on 115,528 measurements), reflecting the larger scatter at the levels omitted from Fig. 4. Considering data only from the Arctic or only from the Antarctic produces *B* estimates that differ only slightly (<0.5%), suggesting that the possibility of incomplete chlorine activation in the Arctic has not significantly compromised our results. Applying a more restrictive definition of “nighttime” for the MLS ClO measurements also has a negligible impact on the overall *B* estimate, as does using a higher threshold temperature to define “warm” conditions. Reducing the assumed value of ClO_x by 30% decreases the estimate of *B* by ~80 K (~0.9%) at these levels in the Arctic (less in the Antarctic). A potential error of 1 K in the temperatures influences *B* at the 45-K level. Bias and scaling errors (1-σ) in the MLS ClO data of 0.05 ppbv and 10% (25), respectively, give rise to uncertainty in *B* of 80 K. Finally, a 0.05-ppbv uncertainty in the latitude- and altitude-dependent empirical bias correction for the version 2 MLS ClO measurements at the lowest retrieval levels (25; also see *Methods*) leads to changes in the retrieved *B* value of ~55 K. Taking the root sum square of the changes in *B* arising from 1-σ estimated uncertainties in the MLS ClO data (80 K), SLIMCAT ClO_x abundances (80 K), MLS ClO bias correction (55 K), temperatures (45 K), SZA threshold (12 K), and included pressure levels (10 K), we estimate the total uncertainty in our retrieved *B* value to be ±135 K. Fig. 4 shows that this uncertainty encompasses all of the variability in the daily *B* retrievals in the Arctic, and nearly all of it in the Antarctic, confirming the validity of our 1-σ uncertainty estimate.

Our overall retrieved *B* values are compared to those recommended in the JPL06 and JPL09 evaluations in Table 4; the corresponding *K*_{eq} values calculated from them at temperatures of 298 and 200 K are also tabulated. The difference between our estimated *B* and that in the recommendation is approximately halved for JPL09 compared to JPL06 (although the derived *K*_{eq} value at 200 K is virtually indistinguishable in the two cases). Consistent with previous studies based on both in situ (3, 5–10) and remote (11) measurements, which have found that *K*_{eq} values

2–6 times smaller than recommended in JPL06 (or earlier evaluations) are required to match atmospheric observations (10), our *B* retrieval yields a value of *K*_{eq} that is smaller than that in JPL09 (JPL06) by a factor of ~1.4 (factor of 2) at temperatures relevant for the polar lower stratosphere.

The temperature dependence of the equilibrium constant ([ClOOCl]/[ClO]²) inferred from the MLS measurements is shown in Fig. 5, along with the *K*_{eq} calculated using the *B* retrieved from the aggregate dataset with *A* fixed to the JPL09 value. The uncertainty range of our derived *K*_{eq} overlaps with that of the JPL09 evaluation. Despite the fact that the laboratory experiments were conducted in temperature regimes very different from those under which the satellite measurements were obtained, the results are largely congruent, validating the extrapolation of the high-temperature laboratory results to lower stratospheric conditions.

Fig. 5 also shows the *K*_{eq} expressions deduced from in situ measurements of ClO in darkness in the perturbed Arctic winter polar vortices of 1990 (6) and 2003 (8). As noted earlier in connection with Figs. 2 and 3, the *K*_{eq} parameterization derived in ref. 8 does not provide a good fit to the MLS data [nor to other published *K*_{eq} values (9)]. Lack of equilibrium or low biases in the simultaneously obtained ClOOCl measurements may have undermined their results (9). In contrast, the analysis of Avallone and Toohey (6) matches that based on MLS data very well, with *K*_{eq} values derived from the two datasets agreeing to within ~5% at lower stratospheric temperatures (for the JPL09 case). Direct intercomparison of measurements with such vastly different sampling scales (satellite data represent “average” conditions over a relatively large volume of air, whereas in situ data represent conditions at a local point) is hampered by atmospheric variability (e.g., ref. 25). Derivation of a fundamental parameter such as *K*_{eq} provides an indirect means of cross-validating datasets obtained two decades apart using completely different techniques. The excellent agreement demonstrated in Fig. 5 further substantiates the quality and quantitative utility of MLS ClO data.

Compared to earlier studies, including of satellite data (11), our analysis has utilized far more measurements, from multiple winters in both hemispheres, and covered higher solar zenith angles in a broad temperature domain. We find that the

Table 4. Overall retrieved *B* values and corresponding *K*_{eq} estimates compared to JPL evaluation values

	<i>B</i> /K	<i>K</i> _{eq} , 298 K	<i>K</i> _{eq} , 200 K
JPL06 (<i>A</i> = 9.30 × 10 ⁻²⁸ cm ³ molecule ⁻¹)*	8,835 ± 300	7.0 + 1.4/ - 1.2 × 10 ⁻¹⁵	1.4 + 1.4/ - 0.7 × 10 ⁻⁸
This study (based on JPL06 <i>A</i> value) [†]	8,694 ± 135	4.4 + 2.6/ - 1.6 × 10 ⁻¹⁵	0.7 + 0.7/ - 0.4 × 10 ⁻⁸
JPL09 (<i>A</i> = 1.72 × 10 ⁻²⁷ cm ³ molecule ⁻¹)*	8,649 ± 200	6.9 + 1.7/ - 1.4 × 10 ⁻¹⁵	1.0 + 0.8/ - 0.4 × 10 ⁻⁸
This study (based on JPL09 <i>A</i> value) [†]	8,570 ± 135	5.3 + 3.2/ - 2.0 × 10 ⁻¹⁵	0.7 + 0.7/ - 0.4 × 10 ⁻⁸

*Uncertainty in *B* given in JPL06 (2). Uncertainty in calculated *K*_{eq} derived by multiplying and dividing by the 1-σ uncertainty factor given in JPL06.

[†]Based on retrieval of the aggregate dataset comprised of 37,272 nighttime MLS ClO measurements at 46 and 68 hPa in the Arctic and 32 and 46 hPa in the Antarctic. Uncertainty on *B* estimated as described in the text. Uncertainty in *K*_{eq} derived by propagating the estimated uncertainty in *B* through the calculation of *K*_{eq}.

[‡]Uncertainty in *B* given in JPL09 (14). Uncertainty in calculated *K*_{eq} derived by multiplying and dividing by the 1-σ uncertainty factor given in JPL09.

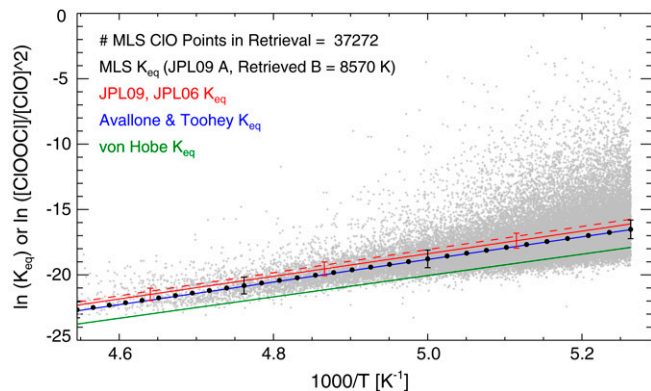


Fig. 5. Inferred equilibrium constant ($[ClOOC]/[ClO]^2$, based on nominal SLIMCAT ClO_x) as a function of reciprocal temperature for 37,272 MLS measurement points meeting the EqL, SZA, and temperature criteria on each day during the peak chlorine activation periods at 32 and 46 hPa in four Antarctic winters and at 46 and 68 hPa in three Arctic winters (small gray crosses). K_{eq} ($=A \times \exp(B/T)$) calculated from the B value retrieved from the aggregate MLS dataset and the JPL09 A value is shown by the large black dots; the range in K_{eq} arising from the estimated uncertainty in the retrieved B (± 135 K) is marked by error bars. The temperature dependence of the inferred K_{eq} is compared to that of the JPL09 expression [red solid line, with the stated uncertainty (14) shown by error bars]. For reference, the JPL06 K_{eq} is also included (red dashed line; the uncertainty range is omitted for clarity). The temperature dependence of the K_{eq} expressions deduced from the in situ measurements of Avallone and Toohey (6) and von Hobe et al. (8) are also shown (blue and green solid lines, respectively).

temperature dependence of the observed nighttime ClO is consistent with thermal equilibrium between ClO and ClOCl.

Methods

MLS measures millimeter- and submillimeter-wavelength thermal emission from the limb of Earth's atmosphere (26). The Aura MLS fields of view point in the direction of orbital motion and vertically scan the limb in the orbit

plane, leading to data coverage from 82°S to 82°N latitude on every orbit. The Aura orbit is sun-synchronous (with an ascending equator-crossing time of 1:45 PM local solar time); thus MLS observations at a given latitude on one segment of the orbit (either ascending or descending) have essentially the same local solar time. Southern high latitudes are sampled by descending measurements near midnight local time, whereas northern high latitudes are sampled by descending measurements in the early predawn hours (~3–5 AM). Here we use version 2.2 (v2.2) MLS ClO measurements, which in the lower stratosphere have vertical resolution of ~3 km. Horizontal resolution is ~3 km across-track and 400–500 km along-track, with ~165 km along-track separation between adjacent profiles (25). Single-profile measurement precision is 0.1 ppbv. The v2.2 MLS ClO data are characterized by a bias uncertainty of ± 0.05 ppbv and a scaling uncertainty of $\pm 10\%$ (1- σ estimates) (25). Because a significant negative bias (0.02–0.27 ppbv) is present in the v2.2 MLS ClO data at the retrieval levels primarily used here, it is necessary to correct individual ClO measurements by subtracting the estimated latitude-dependent value of the negative bias at each of the affected retrieval levels (25).

SLIMCAT is a three-dimensional off-line chemical transport model that includes a detailed description of stratospheric chemistry (22, 27). Photochemical data are taken from the JPL03 recommendation (28), except for the ClOCl photolysis rate, for which the values of ref. 29 are used, with a long-wavelength extrapolation to 450 nm (7). Near-real-time operational SLIMCAT simulations are available for almost every day of MLS data, with an equivalent model value obtained for each MLS observation point, interpolated to the MLS location and taken at the nearest available time (always within 15 min).

MLS and SLIMCAT data are interpolated to potential temperature surfaces and segregated by equivalent latitude using derived meteorological products (30) based on NASA's Global Modeling and Assimilation Office Goddard Earth Observing System versions 5.0.1 and 5.1.0 (GEOS-5) analyses (31).

ACKNOWLEDGMENTS. Thanks to M. P. Chipperfield for developing and sharing the SLIMCAT model and to R. S. Harwood for providing production runs of SLIMCAT for every day of MLS data. Thanks to G. L. Manney and W. H. Daffer for development and production of the MLS derived meteorological products. We are grateful for an extremely insightful and constructive review. Work at the Jet Propulsion Laboratory, California Institute of Technology, was done under contract with the National Aeronautics and Space Administration.

- World Meteorological Organization (WMO) (2007) *Scientific assessment of ozone depletion: 2006* Global Ozone Res. and Monit. Proj. Rep. 50, Geneva.
- Sander SP, et al. (2006) *Chemical kinetics and photochemical data for use in atmospheric studies: Evaluation number 15* Tech Report JPL Publ.06-2 (Jet Propulsion Laboratory).
- Brune WH, Toohey DW, Anderson JG, Chan KR (1990) In situ observations of ClO in the Arctic stratosphere: ER-2 aircraft results from 59°N to 80°N latitude. *Geophys Res Lett* 17:505–508.
- Cox RA, Hayman GD (1988) The stability and photochemistry of dimers of the ClO radical and implications for Antarctic ozone depletion. *Nature* 332:796–800.
- Pierson JM, et al. (1999) An investigation of ClO photochemistry in the chemically perturbed Arctic vortex. *J Atmos Chem* 32(1):61–81.
- Avallone LM, Toohey DW (2001) Tests of halogen photochemistry using in situ measurements of ClO and BrO in the lower polar stratosphere. *J Geophys Res* 106:10411–10421.
- Stimpfle RM, Wilmouth DM, Salawitch RJ, Anderson JG (2004) First measurements of ClOCl in the stratosphere: The coupling of ClOCl and ClO in the Arctic polar vortex. *J Geophys Res* 109:D03301 10.1029/2003JD003811.
- von Hobe M, et al. (2005) A re-evaluation of the ClO/Cl₂O₂ equilibrium constant based on stratospheric in-situ observations. *Atmos Chem Phys* 5:693–702.
- von Hobe M, et al. (2007) Understanding the kinetics of the ClO dimer cycle. *Atmos Chem Phys* 7:3055–3069.
- Schofield R, et al. (2008) Polar stratospheric chlorine kinetics from a self-matched flight during SOLVE-II/EUPLEX. *Geophys Res Lett* 35:L01807 10.1029/2007GL031740.
- Berthet G, et al. (2005) Nighttime chlorine monoxide observations by the Odin satellite and implications for the ClO/Cl₂O₂ equilibrium. *Geophys Res Lett* 32:L11812 10.1029/2005GL022649.
- Plenge J, et al. (2005) Bond strength of chlorine peroxide. *J Phys Chem A* 109:6730–6734.
- Bröske R, Zabel F (2006) Thermal decomposition of ClOCl. *J Phys Chem* 110:3280–3288.
- Sander SP, et al. (2009) *Chemical kinetics and photochemical data for use in atmospheric studies: Evaluation number 16* Tech Report JPL Publ.09-31 (Jet Propulsion Laboratory).
- Nickolaisen SL, Friedl RR, Sander SP (1994) Kinetics and mechanism of the ClO + ClO reaction: Pressure and temperature dependences of the bimolecular and termolecular channels and thermal decomposition of chlorine peroxide. *J Phys Chem* 98:155–169.
- Butchart N, Remsberg EE (1986) The area of the stratospheric polar vortex as a diagnostic for tracer transport on an isentropic surface. *J Atmos Sci* 43:1319–1339.
- Santee ML, et al. (2008) A study of stratospheric chlorine partitioning based on new satellite measurements and modeling. *J Geophys Res* 113:D12307 10.1029/2007JD009057.
- MacKenzie IA, Harwood RS, Froidevaux L, Read WG, Waters JW (1996) Chemical loss of polar vortex ozone inferred from UARS MLS measurements of ClO during the Arctic and Antarctic late winters of 1993. *J Geophys Res* 101:14505–14518.
- Pope FD, Hansen JC, Bayes KD, Friedl RR, Sander SP (2007) Ultraviolet absorption spectrum of chlorine peroxide, ClOCl. *J Phys Chem A* 111:4322–4332.
- von Hobe M (2007) Revisiting ozone depletion. *Science* 318:1878–1879.
- Chen HY, Lien CY, Lin WY, Lee YT, Lin JJ (2009) UV absorption cross sections of ClOCl are consistent with ozone degradation models. *Science* 324:781–784.
- Chipperfield MP (2006) New version of the TOMCAT/SLIMCAT off-line chemical transport model: Intercomparison of stratospheric tracer experiments. *Q J Roy Meteor Soc* 132:1179–1203.
- Chipperfield MP, Feng W, Rex M (2005) Arctic ozone loss and climate sensitivity: Updated three-dimensional model study. *Geophys Res Lett* 32:L11813 10.1029/2005GL022674.
- Feng W, et al. (2005) Three-dimensional model study of the Arctic ozone loss in 2002/2003 and comparison with 1999/2000 and 2003/2004. *Atmos Chem Phys* 5:139–152.
- Santee ML, et al. (2008) Validation of the Aura Microwave Limb Sounder ClO measurements. *J Geophys Res* 113:D15522 10.1029/2007JD008762.
- Waters JW, et al. (2006) The Earth Observing System Microwave Limb Sounder (EOS MLS) on the Aura satellite. *IEEE T Geosci Remote* 44:1075–1092.
- Chipperfield MP (1999) Multiannual simulations with a three-dimensional chemical transport model. *J Geophys Res* 104:1781–1805.
- Sander SP, et al. (2003) *Chemical kinetics and photochemical data for use in atmospheric studies: Evaluation number 14* Tech Report JPL Publ.02-25 (Jet Propulsion Laboratory).
- Burkholder JB, Orlando JJ, Howard CJ (1990) Ultraviolet-absorption cross-sections of Cl₂O₂ between 210 and 410 nm. *J Phys Chem* 94:687–695.
- Manney GL, et al. (2007) Solar occultation satellite data and derived meteorological products: Sampling issues and comparisons with Aura MLS. *J Geophys Res* 112:D24550 10.1029/2007JD008709.
- Reinecker MM, et al. (2008) *The GEOS-5 data assimilation system: A documentation of GEOS-5.0* Tech Report 104606 V27 (NASA).